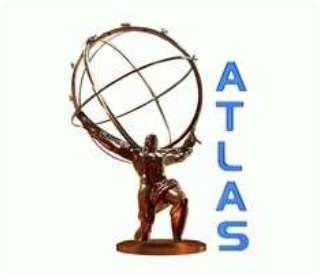

ATLAS NOTE

ATL-COM-TILECAL-2008-?

June 16, 2008

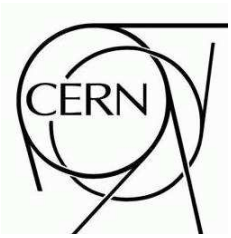

Time Calibration of TileCal Modules with Cosmic Muons

ATL-TILECAL-PUB-2008-010

17 August 2008

Luca Fiorini, Ilya Korolkov, Francesc Vives

IFAE (Barcelona)
contact: fvives@ifae.es

Abstract

A method to synchronize TileCal readout in time using cosmic muons has been developed. It is based on the comparison between the expected time of flight of muons crossing TileCal cells and the measured time. The method has been applied to cosmic data from September and October of 2007, when different sub-detectors of ATLAS were integrated during the Milestone Weeks. The resolution reached with this method is better than 0.7 ns when the statistical error is not the main contribution to the uncertainty.

1 Introduction

The Tile Calorimeter (TileCal) [1] is the main hadronic calorimeter of ATLAS [2], and its principal function is to contribute to the energy reconstruction of the jets produced in the p-p interactions and to the E_T^{miss} measurement. TileCal is located in the region $|\eta| < 1.7$, extending radially from an inner radius of 2.28 m to an outer radius of 4.25 m. It is divided into three cylindrical sections in the z-axis, called Long Barrel (LB) and Extended Barrels (EBs). The LB covers the region $-1.0 < \eta < 1.0$, and the EBs cover the region $0.8 < |\eta| < 1.7$. The LB is divided in two parts, the middle being at $\eta = 0$. Each one of the four parts of TileCal is called partition and the symbols A and C are used to identify them depending if they are in the positive or negative η side respectively. Therefore, the four partitions are EBC, LBC, LBA and EBA, being each one divided in 64 modules in ϕ.

TileCal is made out of steel and scintillating tiles, as absorber and active material respectively. The absorber structure is a laminate of steel plates of various dimensions, connected to a massive structural element referred to as a girder, which is placed at the outer part of the calorimeter. The Tile scintillator plates are placed perpendicular to the colliding beam axis, and are also radially staggered in depth. The structure is periodic along the beam axis. The laminated structure of the absorber allows for grooves in which the wave-length shifting (WLS) fibers run. A compact electronics readout is housed in the girder of each module. The geometry of TileCal cells is defined by arranging the fiber readout in space, creating a quasi-projective tower structure, where the deviations from perfect projectivity are small compared to the typical angular extent of hadronic jets. The readout of the two sides of each scintillating tile of a cell by two separated photomultipliers (PMTs) guarantees a sufficient light yield and aims for redundancy in the read-out. In the PMTs, light produced by particles crossing the tiles is transformed into an analog signal, that is sampled and digitized by the TileCal digitizer system. The samples are processed online by the Optimal Filtering algorithm, that reconstructs the energy amplitude and the phase.

The motivation of the analysis presented is to contribute to the optimization of the reconstructed energy amplitude. The Optimal Filtering algorithm reconstructs the amplitude with a resolution better than 1% when the phase, for a given channel defined as a time difference between the true maximum of the detected signal and closest instance of signal measurement, is known with a resolution of at least 2 ns [3]. Such requirement is due to the fact that the Optimal Filtering algorithm is based on Taylor expansions around the phase value. When the p-p collisions will begin in the LHC and the LVL1 accept rate will exceed 50kHz, only the energy amplitudes and the phases will be stored. Therefore, it is important to achieve optimal time calibration of the detector and to reduce uncertainties in the measurements of the signal amplitudes resulting from poorly defined phases.

The analysis makes use of cosmic muons that cross TileCal. Cosmic muons are mainly produced in decays of Cosmic Rays mesons [4] high in the atmosphere (typically at 15 km above the sea level). Most of the cosmic muons have direction close to the perpendicular to the Earth surface. In order to have muon signals in all TileCal modules, this feature must be taken into account when selecting the kind of trigger the data analyzed was taken with. The TileCal trigger requires a signal above certain energy threshold in one tower in the top side of TileCal and in another in the bottom one. Given the quasi-projective structure of the towers only muons crossing vertical modules are triggered upon. For this reason, the data sample the method has been applied to was triggered by the Resistive Plate Chambers (RPCs) of the Muon Spectrometer. Due to the fact that the RPCs and TileCal are concentric, muons crossing any module of TileCal are selected by the RPC trigger (Fig. 1). For this reason, the method has been applied to data from the periods when the different ATLAS sub-detectors were integrated, known as Milestone Weeks, and when the RPC based trigger was active.

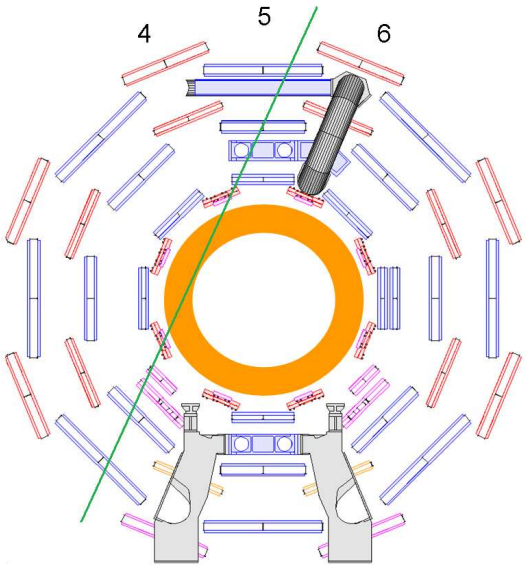

Figure 1: Schema of the RPC trigger. The green line represents a muon crossing horizontal TileCal modules (in orange). The numbers refer to different sectors of the Muon Spectrometer.

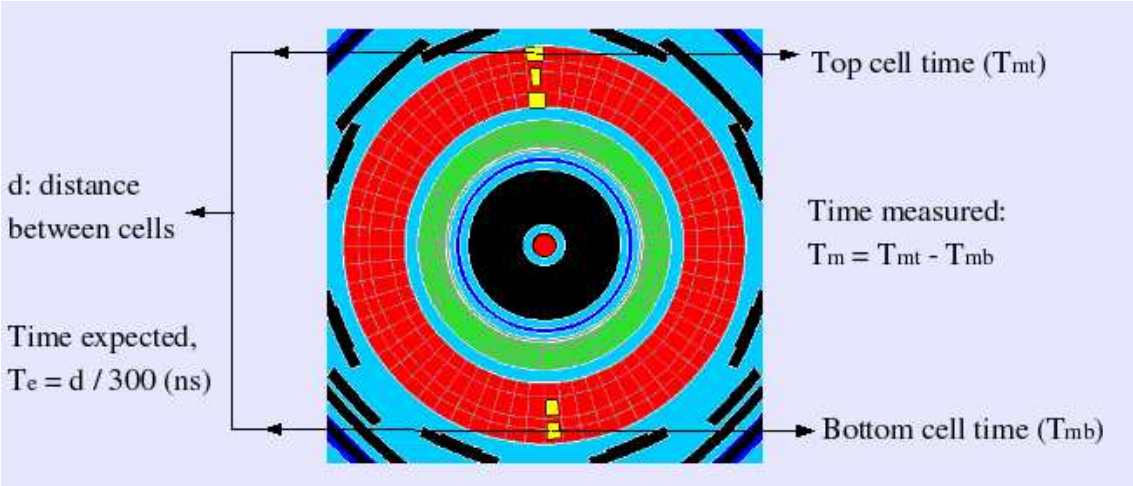

Figure 2: Schema of the method showing two TileCal modules with cells passing the selection criteria (in yellow): the expected time of flight minus the measured one between each pair of cells is what is used to calculate the Time Corrections.

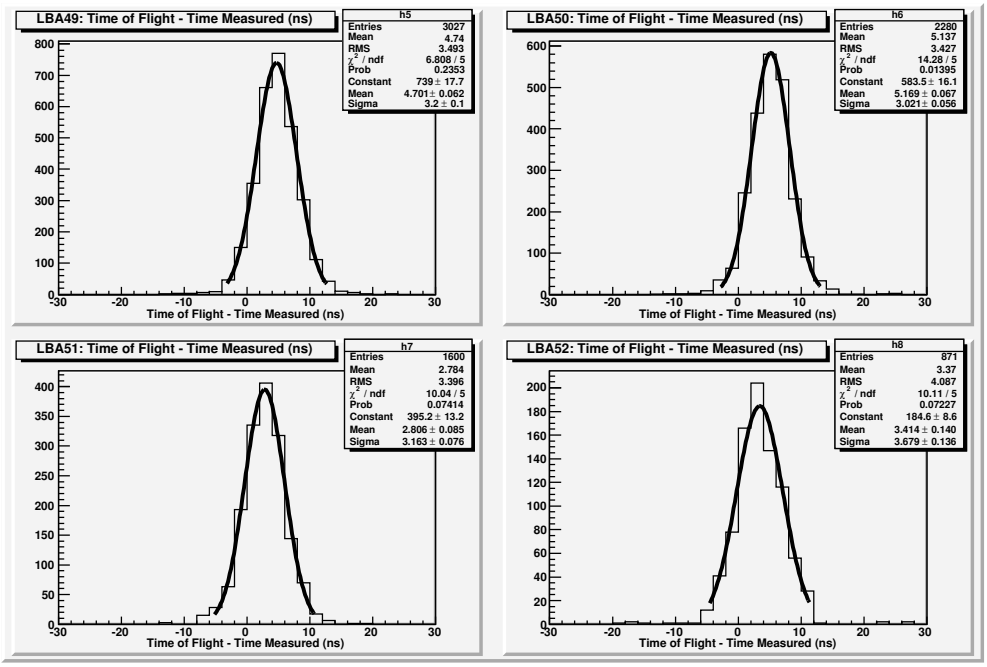

Figure 3: Example of four distributions obtained taking the top module LBA16 as reference, and using muons going from it to the bottom modules LBA49-LBA52. The peaks of the gaussian distribution are the Time Corrections for the bottom modules.

2 Method of calculating the Time Corrections between TileCal modules

The method can be explained considering just two TileCal modules, one at the top and other at the bottom part of the calorimeter. The one at the top is taken as reference. Every stored event is scanned for a muon crossing both modules (Fig. 2) using the selection criteria explained in the next section. Then, for all the possible combinations of pairs of cells crossed by a muon, one in the top module and other in the bottom one, the difference in signal arrival time and the distance between these two cells is calculated. Given that muons detected in TileCal are traveling at a speed close to the speed of light, the expected time of flight is calculated using the distance between the center of the cells. After that, the difference between the expected time of flight of the muon and the measured one is calculated. This is done for each event in the run, and the distribution obtained after the process is fitted with a gaussian function in a range[1)] of ± 8 ns from the mean of the distribution (Fig. 3). The peak value of the gaussian fit is considered as the **Time Correction** for the bottom module relative to the module chosen on the top of the calorimeter.

In this work, module LBA16 has been taken as reference. This is a central module on the top side of TileCal (Fig. 4). Modules that are not back to back to the reference one are more difficult to calibrate, as the probability that a muon crosses them and the reference module drops sensibly. For this reason, an **iteration process** is done in order to intercalibrate all modules within one partition, as it is illustrated in Fig. 4. Bottom modules back to back to the reference one are calibrated first; then these modules are used to calibrate more modules on the top, and this procedure is repeated until a Time Correction for each module is obtained. It is important to remark that the Time Correction with respect to the reference module is propagated from module to module. At the end, all modules are calibrated with respect to the same reference. Using muons crossing the calibrated partition and a module in another partition, the same technique is applied to intercalibrate modules of different partitions, resulting in all the modules

[1)] When 1.5 times the RMS of the distribution is larger than 8 ns, the range used is ± 1.5RMS.

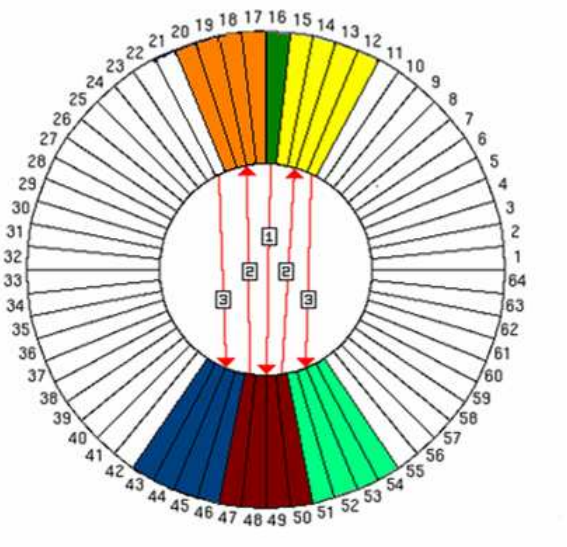

Figure 4: Schema of the first three steps of the iteration process. Modules at the top (bottom) represented with the same color are calibrated with respect to the arbitrary chosen module, as indicated by arrows. The connection with the reference module (in this case module 16) is never lost, and the iteration is continued until all modules are calibrated. The iteration path and the number of modules calibrated together can change during the iteration process. No appreciable difference in the results was found while varying the order of modules in the iteration procedure.

been calibrated against the one chosen as reference.

3 Muon selection criteria

The following selection criteria has been used to define cells crossed by cosmic muons:

1. The **energy** deposition in the cell must be larger than 300 MeV. This is required in order to distinguish muon signals from electronic noise. In particular, it is demanded that each PMT reads at least 150 MeV to exclude possibility that one of the two PMTs gives a large signal due to some electronic or computing problem. For similar reasons it is required that the total energy deposit in the cell must be smaller than 5 GeV. Only a negligible fraction of genuine cosmic muons deposit such energy in TileCal cells and this is yet another handle to exclude cells with readout problems.

2. In the reconstruction process, the time is not reconstructed if the signal is compatible with the electronic noise level. These cases, in which a simplified reconstruction of the signal is performed, are excluded from the analysis.

3. The **difference in time** measured by the two PMTs reading a cell must be smaller than 10 ns. The reason of this requirement is that a muon can take only up to 3.4 ns to cross a cell. Therefore, a difference in time of more than 10 ns indicates that the cell time measurement is not reliable.

Cosmic muons simulated with Monte Carlo methods[2)] were analyzed in order to refine and validate these selection criteria. Using Atlantis, the ATLAS event display program to visualize events, cells with

[2)]The simulation was done in the release 13.0.40 whereas the digitization and the reconstruction in the release 13.0.30.20.

clear muon signal have been found and analyzed individually. This analysis led to the refinement of the first criterion, demanding that the energy readout by each PMT must be larger than 150 MeV, instead of simply requiring that the energy deposition in the cell exceeds 300 MeV. The effectiveness of the other two criteria was also validated on the MC sample.

4 Conditions of cosmic data taken in the Milestone Weeks

Three cosmic runs from the fourth and the fifth Milestone Weeks (M4 and M5) have been analyzed in order to synchronize TileCal modules in time. All runs have an identification number, being 20897 and 20919 the ones corresponding to M4 considered in this case. They were taken between the 1st and the 3rd of September of 2007, lasting 12.5 and 9.5 hours respectively. In the results presented in the next section, 84813 events from run 20897 and 112607 from run 20919 have been analyzed, giving a total of 197420 events from the M4 week. The run number of the M5 week is 29118 and it was 9 hours long, taken the night between the 29th to the 30th of October of 2007. 205374 events of this run have been analyzed. For M4 runs, the trigger rate was $\sim$4 Hz, being the one corresponding to M5 around 2.5 times higher due to the fact that the trigger conditions were different.

During both M4 and M5 periods, the majority of LBA modules and some of LBC modules were in the readout, whereas the full EBA partition was not in the readout during the M4 week. Full EBC partition was not in the readout during the M5 week. The reason for some modules and even entire partitions been not in the readout during these Milestone Weeks is that TileCal was undergoing a refurbishment process of the readout electronics in the partition absent from the readout.

In both cases, during the M4 and M5 weeks, the events were triggered by the RPC. During M4, one of the RPC trigger requirements was that muons pass near the Interaction Point. Given that EBA is more distant than LBA from the Interaction Point, less muons crossing EBA were triggered, in particular $\sim$10 times less than for LBA (Fig. 5(a)). This requirement was not present during the M5 week, and it can be noticed that the distribution of muon signals is similar in all three partitions that were in the readout (Fig. 5(b)) during the M5 week. Another difference in the trigger configuration is that during M4 only RPC stations from the sector 5 of the Muon Spectrometer were triggering, whereas in M5 the RPC stations of sector 6 (Fig. 1) were also included in the trigger. The trigger setup is important for the uniformity of muons collected in TileCal. One can see in Fig. 5, where two plots showing the eta-phi distribution of the TileCal cells crossed by muons in M4 and in M5 runs are presented, that there are factor of $\sim$2.7 more events passing the selection criteria for M4 runs although for this period $\sim$8000 less events were collected. Moreover, in the M5 week the majority of the triggered muons populates the region $x < 0$, that is, where the absolute value of phi is larger than 1.57 rad. Both observations are due to the fact that during M5 the RPC stations of the sector 6 were in the trigger configuration and that it was not required muons passing near the Interaction Point:

1. The geometry of the RPC stations in sector 6 favors the triggering of cosmic muons that do not cross TileCal, specially if they are not demanded to pass near the Interaction Point.

2. The position of the RPCs in the sector 6 favors the collection of muons in the $x < 0$ region, what leads to the concentration of muon signals that one can see in Fig 5(b).

In Fig. 5 plots, it is also shown that there were more cells crossed by muons in the top modules; this is due to the fact that RPC sectors 5 and 6 are on the top side of the ATLAS detector.

The reconstruction of the raw data, which can be found in /castor/cern.ch/grid/atlas/t0/perm/DAQ, has been performed in the release 13.0.30.19. In the reconstruction process, the laser calibration constants in /afs/cern.ch/user/n/ngollub/public/timing/residuals-2007-09-30 have been applied. These constants are intended to calibrate the cells within each module and also the modules within each partition.

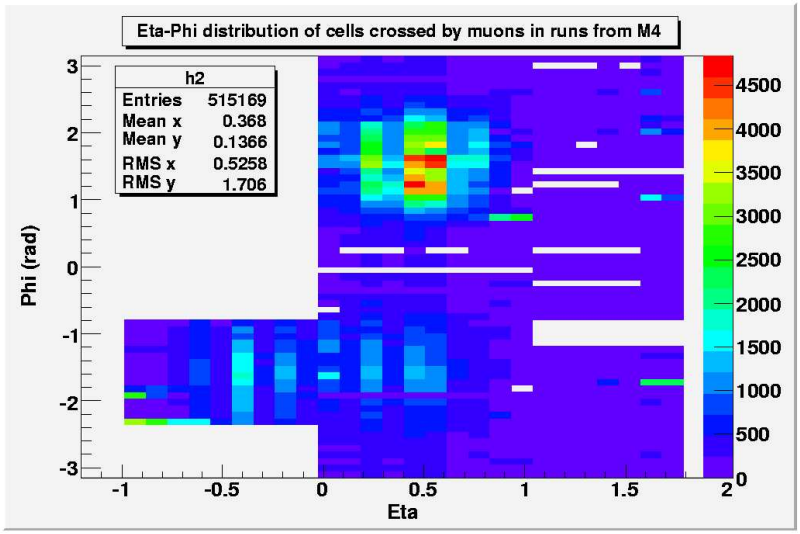

(a) Eta-Phi distribution of TileCal cells crossed by muons in M4 runs 20897 and 20919.

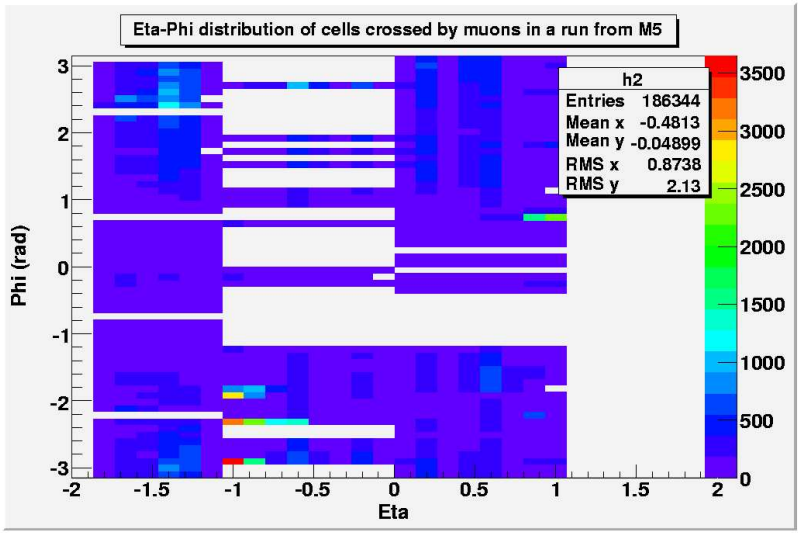

(b) Eta-Phi distribution of TileCal cells crossed by muons in the M5 run 29118.

Figure 5: Eta-Phi distribution of TileCal cells crossed by muons in M4 and in M5 runs.

Therefore, when laser corrections for a module are applied in the reconstruction process, cells within the module can be considered as already synchronized to a good approximation[3)] [5]. In such cases, the time corrections for modules obtained with cosmic muons can also be considered as the correction for each one of its cells. When there are no laser calibration constants available, the time corrections can still be calculated, but they can not be applied to cells individually. Correcting timing for individual cells will require factor of 10 bigger sample of cosmic muons.

5 Results with cosmic data from Milestone Weeks

For EBA and for the Long Barrel partitions, LBA16 has been taken as the reference module. Given the fact that it is in the middle of TileCal top modules, the propagation of the errors is minimized due to the minimization of the number of steps. The reason is that two independent paths are followed to reach the horizontal modules in the two sides of TileCal, one going to larger ϕ values and the other to smaller ones.

EBC has been synchronized only internally, taking EBC28 instead of LBA16 as reference. The reason is that EBC was $\sim$2 m away from LBC during M5, and given the lack of statistics in this period, there are no muons enough crossing both partitions to intercalibrate EBC and LBC partitions.

In this section, the Time Corrections calculated are presented in plots where the error bars include the systematic contribution that will be explained in Section 6. The exact values of the Time Corrections can be found in Appendix A, where statistical and systematic error contributions are showed separately.

5.1 Time Corrections for LBA partition

The Time Corrections obtained with M4 and M5 data for LBA modules are presented in Fig. 6. Results are plotted only for modules in the readout for which laser calibration constants were applied in the reconstruction process. Only for two modules there were no such calibration constants available (LBA04 and LBA45), and they have not been considered together with the other modules for reasons that will be explained in the next section. The Time Corrections for these two modules are given in Appendix A.

One can see that the results obtained with M5 data are different from those obtained with M4 data. This is due to the fact that readout timing setting were changed before the M5 week. The Time Corrections obtained with M5 data have also larger statistical errors, given that the muon statistics is lower for M5 week than for M4 data.

It can be seen that the spread of the Time Corrections obtained with M5 data is larger than the spread of those obtained with M4 data. This is due to the fact that, although the timing of the modules have changed, the laser calibration constants have not; therefore, they were less accurate for M5 data. Given that the laser calibration constants are supposed to synchronize all modules, it is expected that the spread of the Time Corrections is larger for M5 data.

5.2 Time Corrections for LBC partition

The Time Corrections with respect to LBA16 for the LBC modules that were in the readout during M4 and M5 periods are shown in Fig. 7. The same considerations on the variation of the Time Corrections and of their errors between M4 and M5 weeks also apply for LBC.

It is important to remark that there were no laser corrections applied on LBC modules. This can be noticed from the fact that the spread of the Time Corrections is significantly larger than for LBA; they vary from -13.3 ns up to 16.3 ns. In this case, there is no implicit comparison with results obtained by

[3)] The typical uniformity of the phases within a module is $\sim$3 ns before the laser calibration constants are applied, whereas it is reduced to 0.5 ns after applying calibration constants deduced from the laser studies.

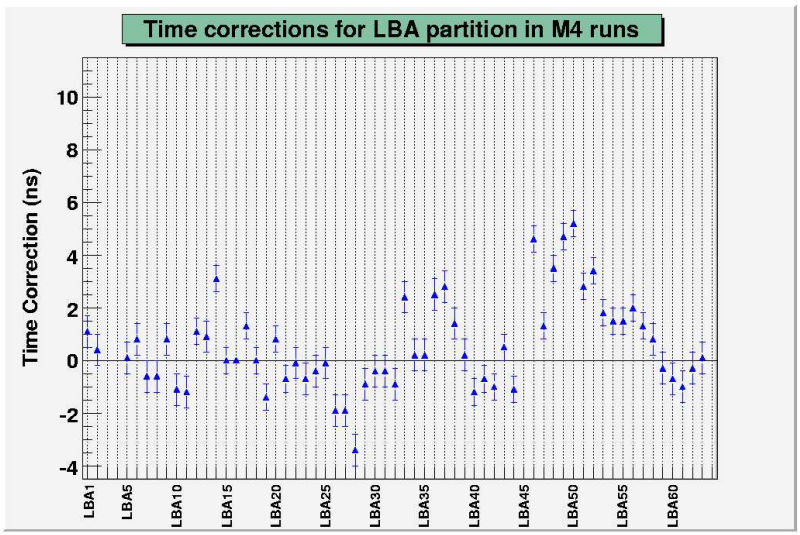

(a) Time Corrections for LBA modules obtained with data from M4 runs.

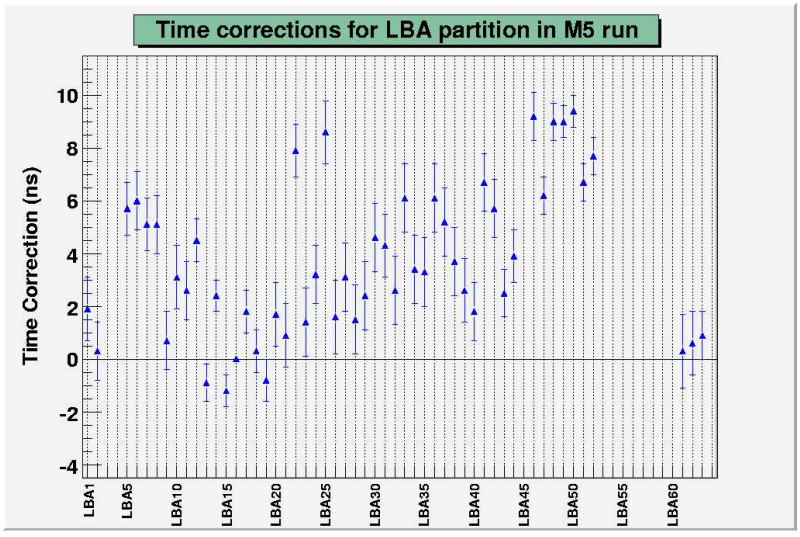

(b) Time Corrections for LBA modules obtained with data from M5 run.

Figure 6: Time Corrections for LBA modules obtained with data from M4 and M5 weeks. Here and in the following Time Corrections plots, the errors plotted also include the systematic ones. In Appendix A, statistical and systematic error contributions are shown separately.

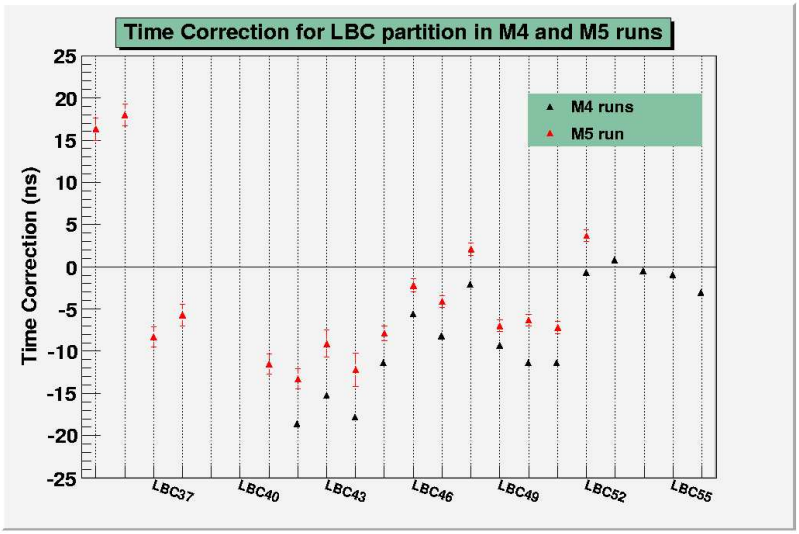

Figure 7: Time Corrections for LBC modules obtained with data from M4 and M5 runs.

the Laser System: the Time Corrections that have been found are the real time shift between modules, without any previous synchronization. It is also the case for LBA04, LBA45, EBA14 and EBC18. The Time Corrections are valid for the modules but the cell to cell variations within these modules are not taken care of.

5.3 Time Corrections for Extended Barrel partitions

The Time Corrections calculated for EBA partition are shown in Fig. 8(a) and those corresponding to EBC partition in Fig. 8(b). It is important to remember that EBC modules were calibrated with respect to EBC28 instead of LBA16, that is the case of the other three partitions. It is interesting to note that, for the two EB partitions, the spread of the Time Corrections is smaller than for LBA, what is in agreement with the results of the Laser System that have also a larger spread for LBA modules calibration constants [6].

Only one half of EBC partition have been analyzed due to the lack of statistics in the remaining modules. The analyzed modules are concentrated in the $x < 0$ region, because it corresponds to the region with better acceptance of the RPC triggers of the sector 6 of the Muon Spectrometer (Section 4).

The delay between EBA16 and LBA16 is shown in Fig. 9, where one can see that this shift is $\sim$24 ns. The reason that there is such large timing difference between partitions is that the laser calibration constants, that have been applied during the reconstruction process in both cases, can not fully account for timing calibration of modules which belong to different partitions. Therefore, although EBA modules were synchronized by the laser system, the method that uses cosmic muons allows to calculate the large time shift between the LBA and the EBA partitions.

6 Systematic errors of the method

Four main sources of the systematic error have been considered:

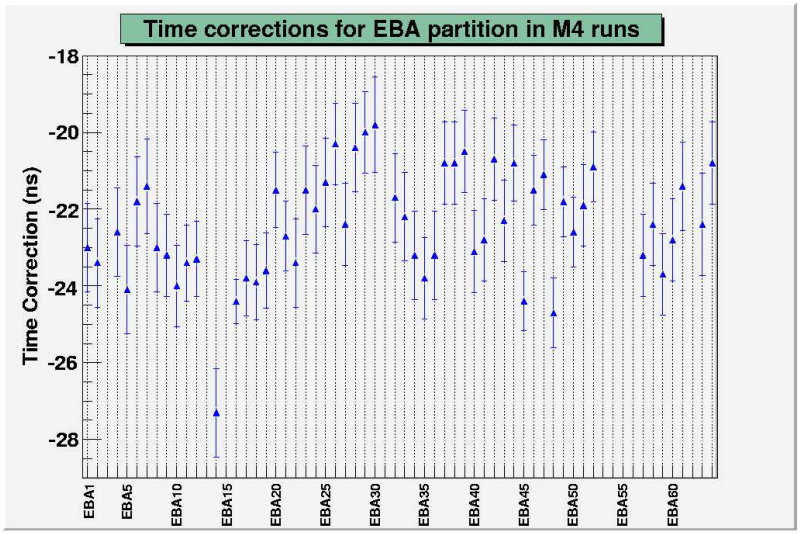

(a) Time Corrections for EBA modules obtained with data from M4 runs. It is important to remember that for EBA14 there were no laser calibration constants to apply during the reconstruction process.

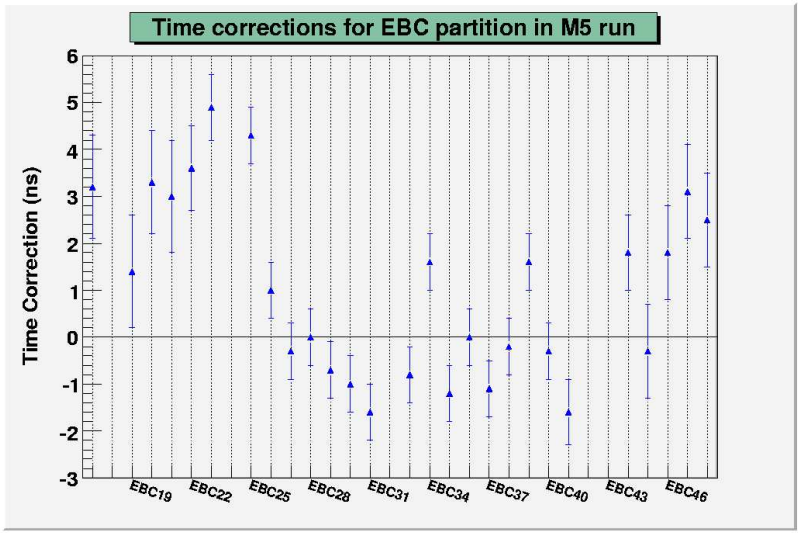

(b) Time Corrections for modules EBC17 to EBC48 obtained with data from M5 run.

Figure 8: Time Corrections for EBA and EBC obtained with data from M4 and M5 respectively.

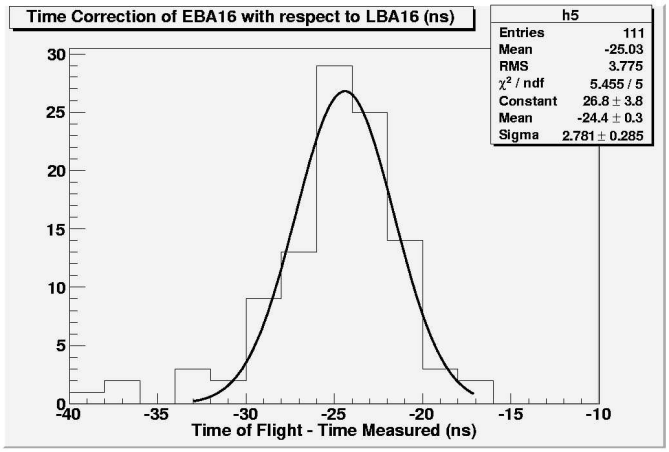

Figure 9: EBA16 Time Correction with respect to LBA16.

1. The Time Correction values are defined as the peaks of the gaussian fit made over the distributions of the difference between the expected time of flight and the measured one. The assumption that the distributions can be fit with a gaussian function may or may not be the case. To evaluate the relevant uncertainty, Time Corrections for LBA modules with M4 data have been calculated using the average value of the distribution in a range of $\pm 3\sigma$, instead of using the peak of the gaussian function. The difference between these Time Corrections and those obtained with the gaussian fit have been calculated and the RMS of the obtained distribution is the systematic error due to this effect (Fig. 10(a)). The value of this error is (0.23 ± 0.02) ns.

2. The method has been applied to a set of simulated cosmic events, where the Time Corrections between modules are expected to be zero by construction. Time Corrections for 111 modules of different partitions have been calculated using 72596 Monte Carlo events. The RMS of the distribution of these Time Corrections has been taken as the contribution to the systematic error due to the imperfect calibration [4)] (Fig. 10(b)). The value of the error after subtracting the statistical contribution is of (0.42 ± 0.03) ns.

3. The contributions to the systematic error due to the variation as a function of time and to the trigger dependence of the results are studied in details in the next section. This contribution is negligible and have not been taken into account.

4. Finally, the systematic error related to the number of steps done in the iteration path have been estimated. Two iteration paths that start and end at the same module and proceed through the same modules (but with opposite directions) have been looked at:

$$\text{LBA16} \rightarrow \left\{ \begin{array}{l} \text{LBA49} \rightarrow \text{LBA17} \rightarrow \text{LBA48} \\ \text{LBA48} \rightarrow \text{LBA17} \rightarrow \text{LBA49} \end{array} \right\} \rightarrow \text{LBA16}$$

[4)] There is a feature not yet explained, the Time Corrections of bottom modules with respect to top ones have an asymmetry in the positive region of $\sim$0.4 ns, whereas they are expected to be compatible with 0 ns. This asymmetry leads to the double peak structure of Fig. 10(b) due to the propagation of the Time Corrections.

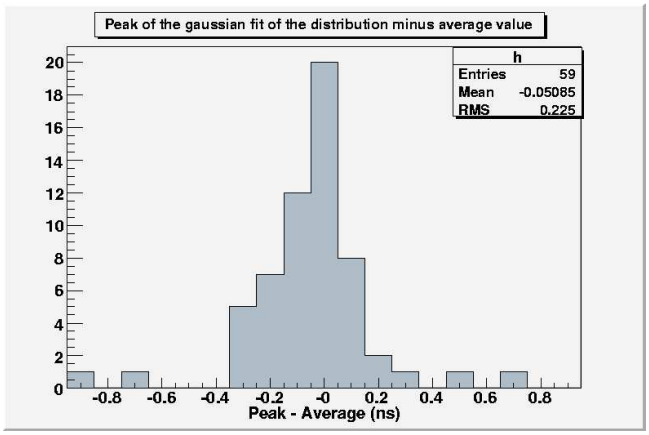

(a) Distribution of the differences between the average of the distribution and the peak of the gaussian fit for LBA modules.

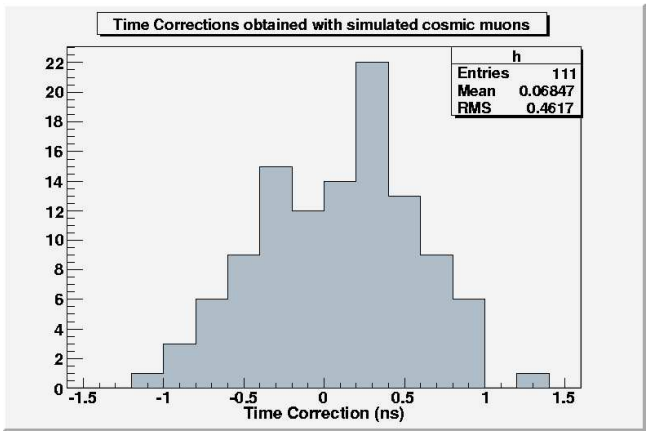

(b) Distribution of Time Corrections obtained with simulated cosmic muons.

Figure 10: Estimation of the two main sources of the systematic error.

Modules with a time difference distribution close to a gaussian function have been chosen, in order not to consider the already evaluated systematic error twice. The difference of the corrections at the end of two iteration paths is expected to be exactly zero by construction, but it is not the case due to the biases introduced by the method, like the binning chosen for the fit of the distribution. The difference between the two final Time Corrections for LBA16 is 0.04 ns, which means a systematic error of 0.02 ns per step in the iteration path. Although this error has been taken into account when the total errors have been calculated, it does not produce sensible effects.

The total systematic error was concluded to be 0.48 ns $\oplus$ 0.02 ns per step in the iteration path.

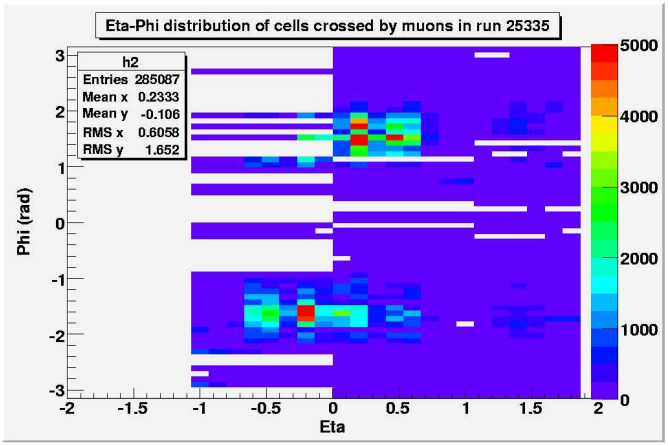

Figure 11: Eta-Phi distribution of TileCal cells crossed by muons in the run 25335.

7 Trigger independence and time stability of the method

In addition to the analysis performed with M4 and M5 data, a run taken between these two periods (run 25335) is compared with runs 20897 and 20919 from the M4 week. The run 25335 was taken on 21th and 23th of September of 2007, collecting 60809 events in 29 hours. All these events have been reconstructed and analyzed. Given the fact that TileCal was operating in stand-alone mode, TileCal towers trigger has been used in order to select muons, instead of the RPC trigger. In Fig. 11, the eta-phi distribution of cells crossed by muons is shown. The main differences between this run and the ones from M4 (Fig. 5(a)) are the following:

- One can see that there are $\sim$2 times less muon signals in run 25335 than in M4 runs by looking at the number of cells passing the selection criteria. All events selected by TileCal trigger are expected to be muons that cross this sub-detector. Considering that run 25335 lasted 7 hours more than the two runs from M4 together, one can conclude that the RPC trigger[5)] is more efficient to collect muons passing through TileCal, because TileCal trigger boards are somewhat noisy.

- It is also possible to observe that the muon signals are concentrated around the region $\phi = \pm 1.5$ rad. As explained in Section 1, this is due to the fact that TileCal trigger makes use of the projective tower structure of the cells, what leads to concentration of the triggers in vertical modules.

In Fig. 12, Time Corrections with respect to LBA16 obtained with data from run 25335 and from M4 runs are compared. They were calculated for all the vertical modules of LBA (Fig. 12(a)) and LBC (Fig. 12(b)) that were in the readout in both runs. One can see that the results are compatible within the error. This agreement is significant especially for the LBC partition, for which no laser calibration constants were available and the cells within each module were not synchronized, as has been explained in Section 5. These results prove the stability of the method in time and also its independence from the trigger used to select muons. For this reason, no systematic uncertainty is attributed neither due to trigger dependence nor due to variation of the results in time. In order to check that the difference in trigger and time of the runs have not opposite effects leading to a cancellation of the resulting bias, data from run

[5)] A muon can cross the RPCs without passing through TileCal because the two detectors are more than 3 m apart.

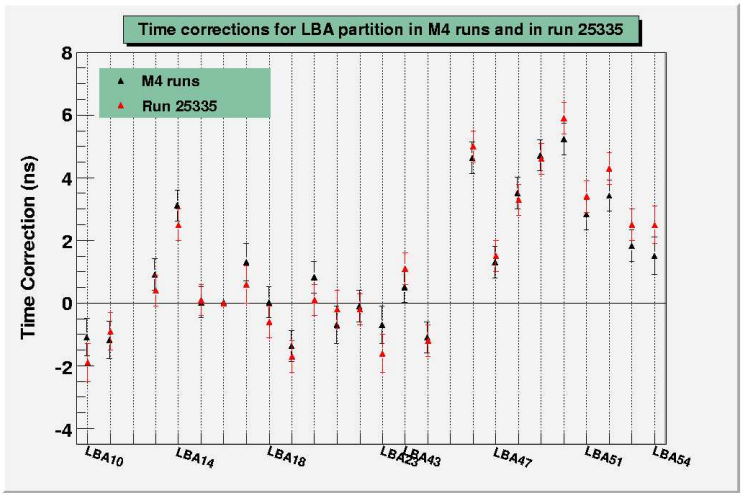

(a) Time Corrections for LBA vertical modules obtained with data from M4 runs and from run 25335. Notice that modules on the top side of TileCal are from LBA10 to LBA23, and that modules from LBA43 to LBA54 are on the bottom side. The errors plotted also include the systematics ones.

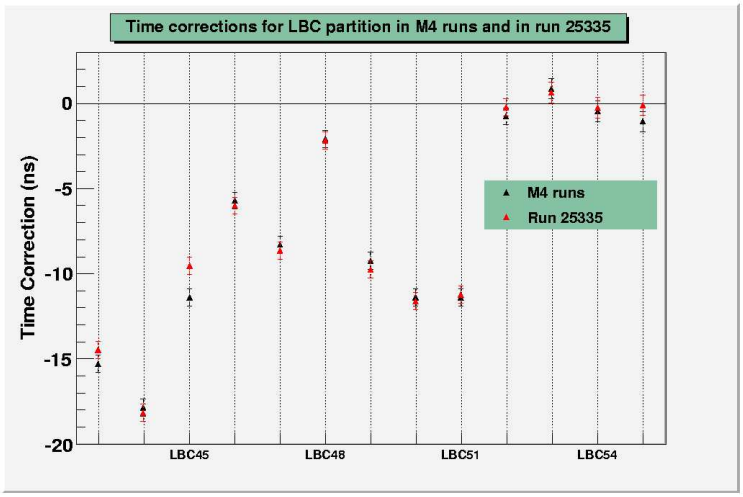

(b) Time Corrections for LBC vertical modules obtained with data from M4 runs and from run 25335. Modules on the top side of TileCal were not in the readout during these runs.

Figure 12: Comparison of Time Corrections obtained with M4 runs and with run 25335.

20897 (M4) triggered by TileCal was compared with data from the same run triggered by the RPCs: the obtained Time Correction results were compatible.

8 Conclusions

A method to synchronize TileCal modules with cosmic muons has been presented. The method is based on comparison of the expected time of flight of muons crossing TileCal to the measured time. The Time Correction value for a module is its timing delay with respect to the module taken as reference once the expected time of flight is taken into account.

Around 400000 events from two Milestone Weeks, M4 and M5, were analyzed. In these Milestone Weeks, the majority of the ATLAS sub-detectors were integrated. In order to have a uniform distribution of muons in all modules, the method was applied to cosmic muons triggered by the RPC stations. The Time Correction values were calculated for all modules available in two Milestone Weeks, which corresponds to 64% of all TileCal modules. All correction values have a precision of at least 2 ns. It is important to remark that, when the sample statistics is such that the statistical error is not the dominant contribution to the uncertainty, a precision better than 0.7 ns is found, as it is the case for LBA partition in the M4 period. This is due to the fact that the systematic error value is of 0.48 ns.

The results of this analysis were compared with the Laser System corrections and the results were found to be fully compatible. The method does not require the laser calibration constants, although they are useful when the statistics is not enough to apply the method to calibrate individual cells directly.

The method could be employed in the future to synchronize directly TileCal cells instead of the modules. Analyzing run 20919 from M4 period, it has been estimated that 5 days of data taking would be enough to calibrate all cells in TileCal, if using the RPC trigger and not requiring muons to pass near the Interaction Point. A possible way to further purify collected muon sample would be to add sectors of the Muon Spectrometer located on the bottom side of ATLAS into the RPC trigger configuration, and to require muons to cross both RPCs sectors, on the top and on the bottom of Tile calorimeter.

The Monte Carlo part of the systematic error is estimated to dominate and to contribute 0.42 ns to the total systematic error. This error includes important contributions from present limitations of the simulation software. Therefore, it is expected that the contribution to the systematic error from the Monte Carlo simulation will be reduced as future versions of the simulation software improves. It has been estimated that this contribution may be reduced in the future by a factor of two.

Sophisticated tools to identify cells crossed by muons have been developed recently [7]. Using them, instead of the muon selection criteria used in this analysis, may lead to more accurate results.

9 Acknowledgements

We would like to thank Christophe Clement, Björn Nordkvist and Nils Gollub for their advices and suggestions about the Laser System timing synchronization; and Sasha Solodkov, Jamie Boyd and Else Lytken for their help in the Monte Carlo simulation of cosmic muons.

References

[1] ATLAS Collaboration: ATLAS Detector and Physics Performance Technical Design Report, CERN/LHCC/99-14,15, 1999 .

[2] ATLAS Collaboration: Tile Calorimeter Technical Design Report, CERN/LHCC/96-42, 1996 .

[3] Belen Salvachua: Online ROD Processing Performance, TileCal Week Data Preparation, October 2007 .

[4] Particle Data Group, Nuclear and Particle Physics, 2006 .

[5] Björn Nordkvist: Synchronization of the ATLAS Hadronic TileCalorimeter Using the Laser Calibration System, Master Thesis, 2007 .

[6] C. Clement et al.: Timing equalization in TileCal, TileCal Week Data Preparation, October 2007 .

[7] Luciano Manhaes De Andrade Filho: Hough Transform method in TileMuonFitter, TileCal Week, February 2008 .

A Tables with Time Corrections

In the previous plots results have been shown with their total errors. In this appendix, the Time Correction values obtained with M4 and M5 data are presented with their statistical errors only. The systematic error is of 0.48 ns plus a negligible contribution of $\sim$0.02 ns per step in the iteration process. One can see that, when the sample statistics is as for LBA and LBC during M4, the total error is always below than 0.7 ns.

Table 1: Time Corrections with respect to EBC 28 for EBC17 to EBC48 modules obtained with M5 data.

Module	**Time Corrections (M5)**	**Module**	**Time Correction (M5)**
EBC17	3.2 $\pm$ 1.0	EBC33	-0.8 $\pm$ 0.2
EBC18	8.4 $\pm$ 1.1	EBC34	1.6 $\pm$ 0.2
EBC19	1.4 $\pm$ 1.1	EBC35	-1.2 $\pm$ 0.2
EBC20	3.3 $\pm$ 1.0	EBC36	0.0 $\pm$ 0.2
EBC21	3.0 $\pm$ 1.1	EBC37	-1.1 $\pm$ 0.2
EBC22	3.6 $\pm$ 0.7	EBC38	-0.2 $\pm$ 0.2
EBC23	4.9 $\pm$ 0.5	EBC39	1.6 $\pm$ 0.3
EBC24	—	EBC40	-0.3 $\pm$ 0.3
EBC25	4.3 $\pm$ 0.3	EBC41	-1.6 $\pm$ 0.5
EBC26	1.0 $\pm$ 0.3	EBC42	—
EBC27	-0.3 $\pm$ 0.3	EBC43	—
EBC28	0.0 $\pm$ 0.3	EBC44	1.8 $\pm$ 0.6
EBC29	-0.7 $\pm$ 0.3	EBC45	-0.3 $\pm$ 0.9
EBC30	-1.0 $\pm$ 0.3	EBC46	1.8 $\pm$ 0.9
EBC31	-1.6 $\pm$ 0.3	EBC47	3.1 $\pm$ 0.9
EBC32	—	EBC48	2.5 $\pm$ 0.9

Table 2: Time Corrections with respect to LBA16 for EBA modules obtained with M4 data.

Module	**Time Corrections (M4)**	**Module**	**Time Correction (M4)**
EBA1	-23.0 $\pm$ 0.9	EBA33	-22.2 $\pm$ 0.9
EBA2	-23.4 $\pm$ 0.9	EBA34	-23.2 $\pm$ 0.9
EBA3	—	EBA35	-23.8 $\pm$ 0.8
EBA4	-22.6 $\pm$ 0.9	EBA36	-23.2 $\pm$ 0.9
EBA5	-24.1 $\pm$ 0.9	EBA37	-20.8 $\pm$ 0.8
EBA6	-21.8 $\pm$ 0.9	EBA38	-20.8 $\pm$ 0.8
EBA7	-21.4 $\pm$ 1.0	EBA39	-20.5 $\pm$ 0.8
EBA8	-23.0 $\pm$ 0.9	EBA40	-23.1 $\pm$ 0.8
EBA9	-23.2 $\pm$ 0.8	EBA41	-22.8 $\pm$ 0.8
EBA10	-24.0 $\pm$ 0.8	EBA42	-20.7 $\pm$ 0.8
EBA11	-23.4 $\pm$ 0.7	EBA43	-22.3 $\pm$ 0.8
EBA12	-23.3 $\pm$ 0.7	EBA44	-20.8 $\pm$ 0.7
EBA13	—	EBA45	-24.4 $\pm$ 0.3
EBA14	-27.3 $\pm$ 0.9	EBA46	-21.5 $\pm$ 0.6
EBA15	—	EBA47	-21.1 $\pm$ 0.6
EBA16	-24.4 $\pm$ 0.3	EBA48	-24.7 $\pm$ 0.6
EBA17	-23.8 $\pm$ 0.7	EBA49	-21.8 $\pm$ 0.6
EBA18	-23.9 $\pm$ 0.7	EBA50	-22.6 $\pm$ 0.6
EBA19	-23.6 $\pm$ 0.7	EBA51	-21.9 $\pm$ 0.8
EBA20	-21.5 $\pm$ 0.7	EBA52	-20.9 $\pm$ 0.6
EBA21	-22.7 $\pm$ 0.6	EBA53	—
EBA22	-23.4 $\pm$ 0.9	EBA54	—
EBA23	-21.5 $\pm$ 0.9	EBA55	—
EBA24	-22.0 $\pm$ 0.9	EBA56	—
EBA25	-21.3 $\pm$ 0.9	EBA57	-23.2 $\pm$ 0.8
EBA26	-20.3 $\pm$ 0.8	EBA58	-22.4 $\pm$ 0.8
EBA27	-22.4 $\pm$ 0.8	EBA59	-23.7 $\pm$ 0.8
EBA28	-20.4 $\pm$ 0.9	EBA60	-22.8 $\pm$ 0.8
EBA29	-20.0 $\pm$ 0.8	EBA61	-21.4 $\pm$ 0.9
EBA30	-19.8 $\pm$ 1.0	EBA62	—
EBA31	—	EBA63	-22.4 $\pm$ 1.1
EBA32	-21.7 $\pm$ 0.9	EBA64	-20.8 $\pm$ 0.8

Table 3: Time Corrections with respect to LBA16 for LBC35 to LBC56 modules obtained with M4 and M5 data.

Module	**Time Correction (M4)**	**Time Correction (M5)**
LBC35	—	16.3 ± 1.3
LBC36	—	18.0 ± 1.4
LBC37	—	-8.3 ± 1.2
LBC38	—	-5.7 ± 1.3
LBC39	—	—
LBC40	—	—
LBC41	—	-11.5 ± 1.2
LBC42	-18.7 ± 0.1	-13.3 ± 1.3
LBC43	-15.3 ± 0.1	-9.1 ± 1.6
LBC44	-17.9 ± 0.1	-12.2 ± 2.0
LBC45	-11.4 ± 0.1	-7.9 ± 0.8
LBC46	-5.7 ± 0.1	-2.2 ± 0.7
LBC47	-8.3 ± 0.1	-4.1 ± 0.4
LBC48	-2.1 ± 0.1	2.1 ± 0.4
LBC49	-9.3 ± 0.1	-7.0 ± 0.4
LBC50	-11.4 ± 0.1	-6.3 ± 0.5
LBC51	-11.4 ± 0.1	-7.2 ± 0.5
LBC52	-0.8 ± 0.1	3.7 ± 0.5
LBC53	0.8 ± 0.3	—
LBC54	-0.5 ± 0.3	—
LBC55	-1.1 ± 0.3	—
LBC56	-3.2 ± 0.3	—

Table 4: Time Corrections with respect to LBA16 for LBA1 to LBA32 modules obtained with M4 and M5 data.

Module	**Time Correction (M4)**	**Time Correction (M5)**
LBA01	1.1 ± 0.2	1.9 ± 1.0
LBA02	0.4 ± 0.2	0.3 ± 0.9
LBA03	—	—
LBA04	—	41 ± 1.1
LBA05	0.1 ± 0.3	5.7 ± 0.9
LBA06	0.8 ± 0.3	6.0 ± 0.9
LBA07	-0.6 ± 0.3	5.1 ± 0.9
LBA08	-0.6 ± 0.3	5.1 ± 0.9
LBA09	0.8 ± 0.2	0.7 ± 0.9
LBA10	-1.1 ± 0.2	3.1 ± 1.1
LBA11	-1.2 ± 0.2	2.6 ± 0.9
LBA12	1.1 ± 0.1	4.5 ± 0.7
LBA13	0.9 ± 0.2	-0.9 ± 0.4
LBA14	3.1 ± 0.1	2.4 ± 0.4
LBA15	0.0 ± 0.1	-1.2 ± 0.4
LBA16	0.0 ± 0.0	0.0 ± 0.0
LBA17	1.3 ± 0.1	1.8 ± 0.6
LBA18	0.0 ± 0.1	0.3 ± 0.6
LBA19	-1.4 ± 0.1	-0.8 ± 0.6
LBA20	0.8 ± 0.1	1.7 ± 1.1
LBA21	-0.7 ± 0.1	0.9 ± 1.1
LBA22	-0.1 ± 0.2	7.9 ± 0.9
LBA23	-0.7 ± 0.2	1.4 ± 1.2
LBA24	-0.4 ± 0.2	3.2 ± 0.9
LBA25	-0.1 ± 0.3	8.6 ± 1.1
LBA26	-1.9 ± 0.3	1.6 ± 1.3
LBA27	-1.9 ± 0.3	3.1 ± 1.2
LBA28	-3.4 ± 0.3	1.5 ± 1.2
LBA29	-0.9 ± 0.3	2.4 ± 1.2
LBA30	-0.4 ± 0.2	4.6 ± 1.2
LBA31	-0.4 ± 0.2	4.3 ± 1.1
LBA32	-0.9 ± 0.2	2.6 ± 1.2

Table 5: Time Corrections with respect to LBA16 for LBA33 to LBA64 modules obtained with M4 and M5 data.

Module	**Time Correction (M4)**	**Time Correction (M5)**
LBA33	2.4 ± 0.2	6.1 ± 1.2
LBA34	0.2 ± 0.2	3.4 ± 1.2
LBA35	0.2 ± 0.3	3.3 ± 1.2
LBA36	2.5 ± 0.2	6.1 ± 1.2
LBA37	2.8 ± 0.2	5.2 ± 1.2
LBA38	1.4 ± 0.2	3.7 ± 1.2
LBA39	0.2 ± 0.2	2.6 ± 1.1
LBA40	-1.2 ± 0.2	1.8 ± 1.0
LBA41	-0.7 ± 0.2	6.7 ± 1.0
LBA42	-1.0 ± 0.2	5.7 ± 1.0
LBA43	0.5 ± 0.2	2.5 ± 0.8
LBA44	-1.1 ± 0.2	3.9 ± 0.8
LBA45	16.0 ± 0.5	—
LBA46	4.6 ± 0.1	9.2 ± 0.7
LBA47	1.3 ± 0.1	6.2 ± 0.5
LBA48	3.5 ± 0.1	9.0 ± 0.4
LBA49	4.7 ± 0.1	9.0 ± 0.2
LBA50	5.2 ± 0.1	9.4 ± 0.3
LBA51	2.8 ± 0.1	6.7 ± 0.4
LBA52	3.4 ± 0.1	7.7 ± 0.5
LBA53	1.8 ± 0.2	—
LBA54	1.5 ± 0.2	—
LBA55	1.5 ± 0.2	—
LBA56	2.0 ± 0.2	—
LBA57	1.3 ± 0.2	—
LBA58	0.8 ± 0.2	—
LBA59	-0.3 ± 0.2	—
LBA60	-0.7 ± 0.2	—
LBA61	-1.0 ± 0.3	0.3 ± 1.3
LBA62	-0.3 ± 0.2	0.6 ± 1.0
LBA63	0.1 ± 0.2	0.9 ± 0.8
LBA64	—	—